



Tsunami Inundation and Maritime Hazard Modelling for a Maximum Credible Tsunami Scenario in Southeast Tasmania, Australia

CLAIRE L. KAIN,¹  BARRIE LEWARN,² EDWARD H. RIGBY,³ and COLIN MAZENGARB¹

Abstract—The east coast of Tasmania is directly exposed to tsunamis originating from the Puysegur subduction zone, off New Zealand’s southwest coast. However, the potential impacts of tsunami inundation for coastal communities and Hobart Airport, and risks to maritime operations in Hobart Port, are poorly understood. The purpose of this project is to simulate a maximum credible earthquake/tsunami/high tide scenario (a Mw 8.7 rupture of the Puysegur subduction zone) across a 17,000 km² model area and provide outputs that can inform local hazard management plans. Modelling was performed using the ANUGA hydrodynamic library, along with a detailed elevation model constructed from LiDAR, photogrammetric contours and bathymetric datasets. The modelling strategy comprised three primary scenarios: a 13 h simulation of tsunami activity focusing on maritime hazard from waves and currents, with two further 4 h simulations focusing on coastal inundation for 71 coastal communities and Hobart Airport. The models were run on a variable triangulated mesh with a detailed Manning’s *n* surface roughness model. Tsunami erosion of sand dunes was accounted for through the development of an erosion operator. Results predict severe inundation (> 4 m flow depth) in exposed east-facing areas and the maritime hazard assessment advises that water disturbance would pose a significant threat to marine craft. The assessment suggests that the feasibility of shipping evacuation from Hobart port is questionable, given the timeframes involved and the nature of simulated water disturbance. Modelling results suggest that the dune line in front of Hobart Airport would not be breached in this instance and so inundation would not occur.

Keywords: Tsunami, modelling, hazard, emergency management.

1. Introduction

The east coast of Australia, including Tasmania, is exposed to tsunamis originating from many source regions around the Pacific Ocean. Southeast Tasmania is particularly exposed to tsunamis originating along the Puysegur subduction zone, located off the southwest coast of New Zealand. Several small tsunamis have been recorded in Tasmania since 1858 (Goff and Chagué-Goff 2014; Morris and Mazengarb 2009; Uslu et al. 2011), but no large events have occurred in recorded history. However, geological evidence suggests the occurrence of several significant tsunami events within the last 4000 years (Clark et al. 2011).

In the absence of eyewitness records of damaging tsunami events, numerical modelling of tsunamis can provide a method of predicting potential impacts and investigating the risk to coastal communities. Initial tsunami modelling for southeast Tasmania was undertaken in 2009 (Van Putten et al. 2009) and results indicated that parts of the coastline could be significantly affected by a tsunami generated from a large rupture of the Puysegur subduction zone, off New Zealand’s southwest coast. Emergency managers have since sought greater detail on potential impacts for coastal communities, infrastructure and operations in Hobart Port.

The impacts of tsunami waves and currents for maritime infrastructure and operations has long been apparent in historical records, yet this aspect of tsunami hazard is commonly neglected (Borrero et al. 2015; Lynett et al. 2014). Following the large tsunamis in recent decades, damage and disruptions were experienced in ports adjacent to the tsunami source region, but also in far-field transoceanic

¹ Mineral Resources Tasmania, PO Box 56, Rosny Park, Hobart 7018, Tasmania, Australia. E-mail: claire.kain@stategrowth.tas.gov.au; colin.mazengarb@stategrowth.tas.gov.au

² Australian Maritime College Search, University of Tasmania, Locked Bag 1400, Launceston 7248, Tasmania, Australia. E-mail: Barrie.lewarn@utas.edu.au

³ Rienco Consulting, PO Box 602, Sorell 7172, Tasmania, Australia. E-mail: ted.rigby@rienco.com.au

locations. For example, the 1960 Chile tsunami caused surging, currents and damage in harbours as far afield as Australia, Japan, New Zealand and Hawaii (Beccari 2009; Cox and Mink 1963; Heath 1976; Kato et al. 1961). Following the 2004 Indian Ocean tsunami, port areas were completely destroyed in Banda Aceh, and tsunami currents caused mooring lines to break and ships to be cast adrift as far away as Madagascar and Reunion Island (Okal et al. 2006a, b). Similarly, the 2011 Tohoku tsunami destroyed port infrastructure along the adjacent coastline, and effects were felt across the Pacific Ocean with coastal erosion and strong currents causing disruption to harbour operations in California (Wisniewski and Wolski 2012). Research has begun to address this gap and numerical models have been developed that are capable of simulating tsunami current speeds, which in conjunction with modelled wave data and coastal inundation mapping can allow an educated assessment of the hazard to maritime operations and infrastructure (e.g. Hasan et al. 2017; Lynett et al. 2012, 2017; Muhari et al. 2015).

The purpose of this work is to model the impacts of a maximum credible earthquake/tsunami/high tide scenario in southeast Tasmania using new high resolution bathymetric and topographic data, and to explore the maritime hazard posed by such an event. The project scope includes an assessment of the risk to the Hobart airport runway and terminal from potential tsunami inundation.

2. Methods

The model scenario represents a maximum credible earthquake/tsunami/high tide combination, which corresponds to a Mw 8.7 earthquake on the Puysegur Subduction Zone. The rupture zone for this scenario covers a length of 425 km and a width of 125 km, with a dip of 15° and slip of 6.65 m. Tsunami source and propagation modelling were performed as part of the first probabilistic tsunami hazard assessment (PHTA) for Australia (Burbidge et al. 2008). This event represents an approximate annual exceedance probability (AEP) of one in 13,000 years. Initially, the AEP of this scenario was calculated as one in 10,000 years, but this has since

been revised. Van Putten et al. (2009) modelled a number of Tasmanian tsunami inundation scenarios at a coarser resolution, in order to explore the effects of different rupture geometries and earthquake magnitudes, and we selected an event that corresponds with this study's 'worst case scenario'.

The model domain covers an area of approximately 17,000 km² (Fig. 1) and the resulting coastal inundation map series covers 71 communities. This area includes greater Hobart, which is Tasmania's largest city and has a population of approximately 232,000 (Australian Bureau of Statistics 2018).

The modelling strategy comprised three scenarios, as follows:

(A) Maritime hazard (13 h simulation).

(B) Coastal inundation (4 h simulation).

(C) Hobart airport hazard and dune erosion modelling (4 h simulation).

Note that the start time of the simulation was 1.4 h post-earthquake, to capture the moment the tsunami arrived at the model boundary and minimise computational time. The 13 h simulated outputs for Scenario A were inspected and a 4 h simulation was deemed sufficient for the higher resolution coastal inundation modelling in Scenarios B and C, as the maximum impacts occurred within this window.

2.1. Input Data Preparation

Four main sets of input data were required to accurately model nearshore tsunami propagation and inundation, including: Boundary condition hydrographs, mesh resolution zones, a digital elevation model and a surface roughness model (Manning's roughness coefficient: n). A polygon shape file was used to specify areas of potential dune erosion.

2.1.1 Boundary Conditions

The boundary condition hydrographs represent the incoming tsunami water level and momentum in deep water (100 m depth contour, Fig. 2). These data are freely available from Geoscience Australia for a range of tsunami rupture and deep water modelling scenarios (Burbidge et al. 2008) and we have taken the levels for the above mentioned event as the inputs to our nearshore modelling. We note that the PHTA

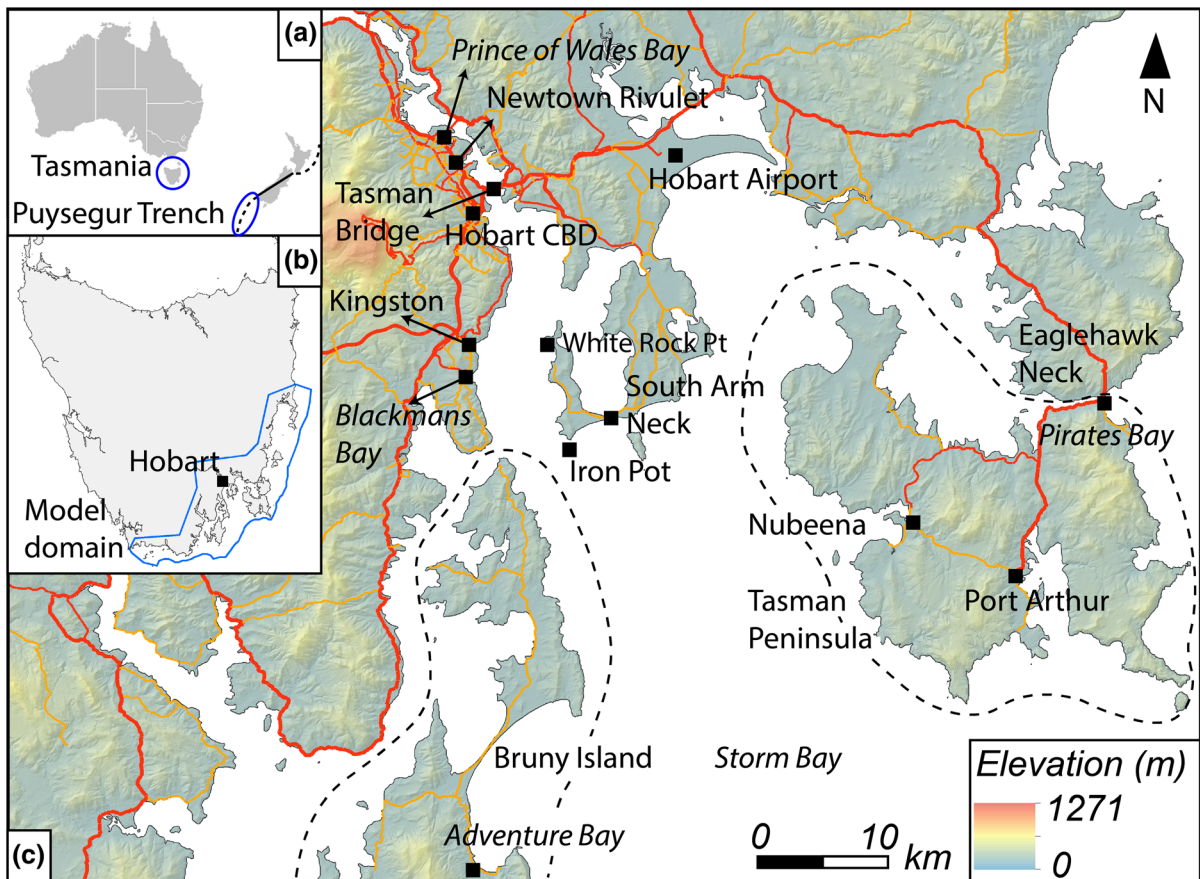


Figure 1

a Location of Tasmania with respect to the Puysegur subduction zone. **b** Coverage of the model domain. **c** Locations of key areas and places mentioned in the text

has been updated since this work was completed (Davies and Griffin 2018). The boundary condition dataset covered a 5 h period, beyond which time the seaward boundary reverted to an initial stage, zero momentum, non-reflective boundary. The top and bottom segments of the domain boundary (i.e. the northernmost and southernmost ocean segments not subject to the time series boundary conditions) were transmissive, thus allowing the waves to exit the domain.

2.1.2 Mesh Resolution

The resolution of the modelling mesh controls the level of detail of the modelling process and outputs; however, processing time increases substantially when a finer mesh is used. An unstructured triangular mesh was employed, to allow variation in mesh

resolution across the irregularly shaped study area. Mesh resolution varies from a 400 m triangular mesh in deep ocean and high land areas to a 10 m triangular mesh in coastal areas of particular interest. Details of the mesh resolution zones are given in Table 1 and Fig. 3.

2.1.3 Elevation Model

A seamless elevation model was constructed by combining bathymetric and topographic data from a variety of sources (Table 2), using the terrain geoprocessing tools in ArcGIS. To avoid introducing artefacts due to overlapping datasets, the datasets were masked so that the newest and/or highest resolution data took precedence in any given location. In addition to the data listed in Table 2, additional elevation points were added at 20 m intervals along

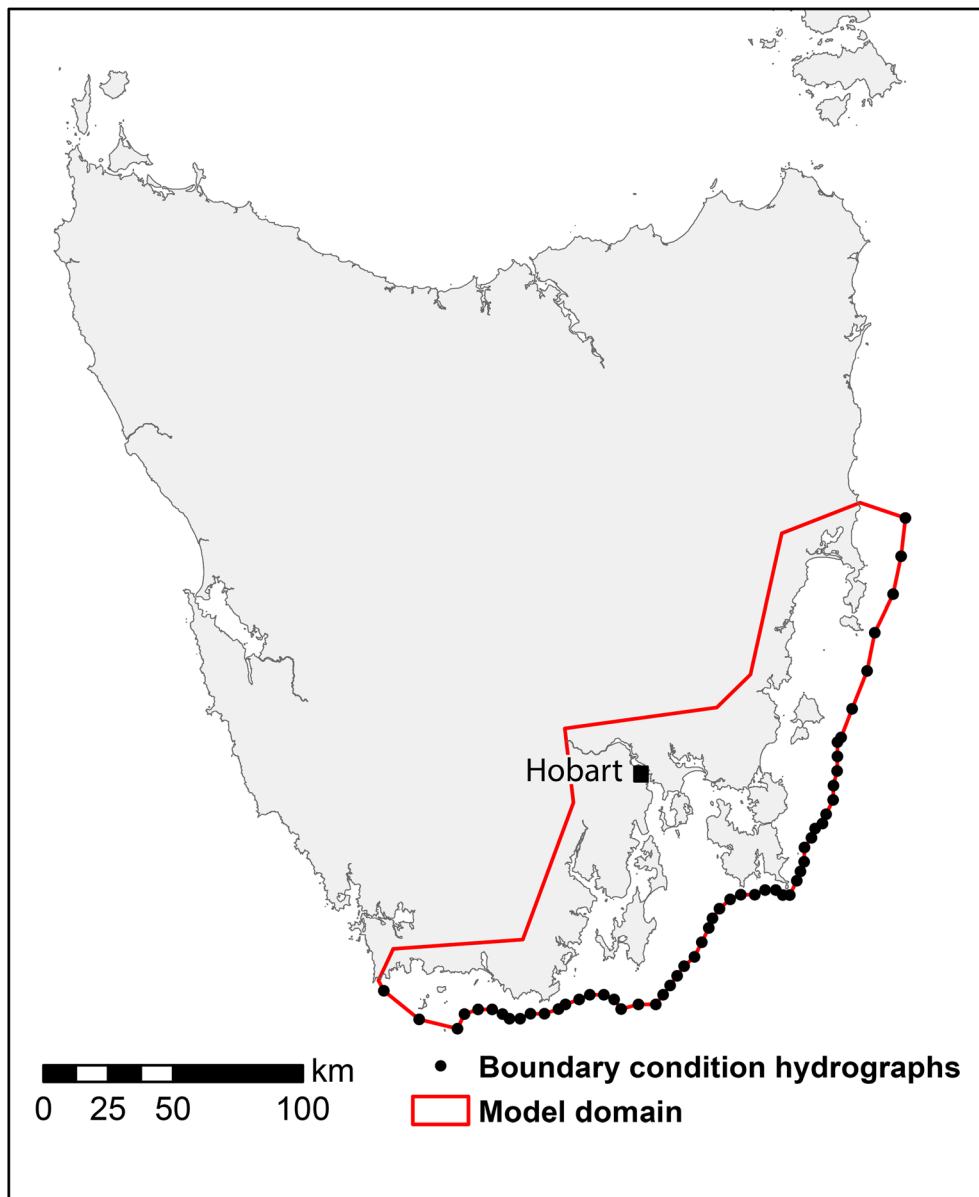


Figure 2
Location of the model domain and boundary condition hydrographs

the mapped coastline (at mean sea level and highest astronomical tide) to ensure the coastal margin was properly constrained.

2.1.4 Mannings n Surface Roughness Model

Surface roughness is an important control on wave attenuation and run-up distances. Factors such as

vegetation cover, rivers and the presence or density of buildings can result in considerable variation in flooding patterns. Variations in surface cover were mapped in ArcGIS and accounted for in the model, using the Manning's n parameter (e.g. Bricker et al. 2015; Chow 1959). A number of publicly available datasets were used to generate the surface map, including the statewide road network, water course

Table 1

Mesh resolution zones and areas covered

Mesh resolution (triangle length, m)	Coverage
Coarse: 400 × 400	Open ocean and land > 15 m ASL
Medium: 200 × 200	Offshore areas – 30 > – 10 m ASL
Fine: 50 × 50	Rural areas – 10 m > 10 m ASL
Very fine: 20 × 20	Urban areas of interest
Extra fine: 10 × 10	Hobart Airport, Blackmans Bay

and cadastre layers (Land Information System Tasmania 2016) and the TASVEG vegetation map (DPIPWE 2013). Building footprints were extracted from the LiDAR data. The Manning's n coefficient for each surface type, as assigned based on the Australian Rainfall and Runoff Guidelines (Commonwealth of Australia—Geoscience Australia

2016), is listed in Table 3 and a spatial representation is given in Fig. 4.

2.2. Modelling Using ANUGA

Modelling was performed using the free and open source ANUGA hydrodynamic modelling library (Nielsen et al. 2005; Roberts et al. 2019). ANUGA was developed by the Australian National University (ANU) and Geoscience Australia (GA) and has been widely used to simulate tsunami inundation since its public release in 2006 (e.g. Baldock et al. 2007; Jakeman et al. 2010; Sterzai et al. 2015; Wilson et al. 2018). Several validation studies have compared ANUGA with other 2D hydrodynamic models or solutions and found the results aligned well (Fernandes 2009; Mungkasi and Roberts 2013), while modelling of historical events has also been undertaken for Sydney Harbour (Wilson et al. 2018) and the model solution found to be within an acceptable level of uncertainty. In addition, inundation

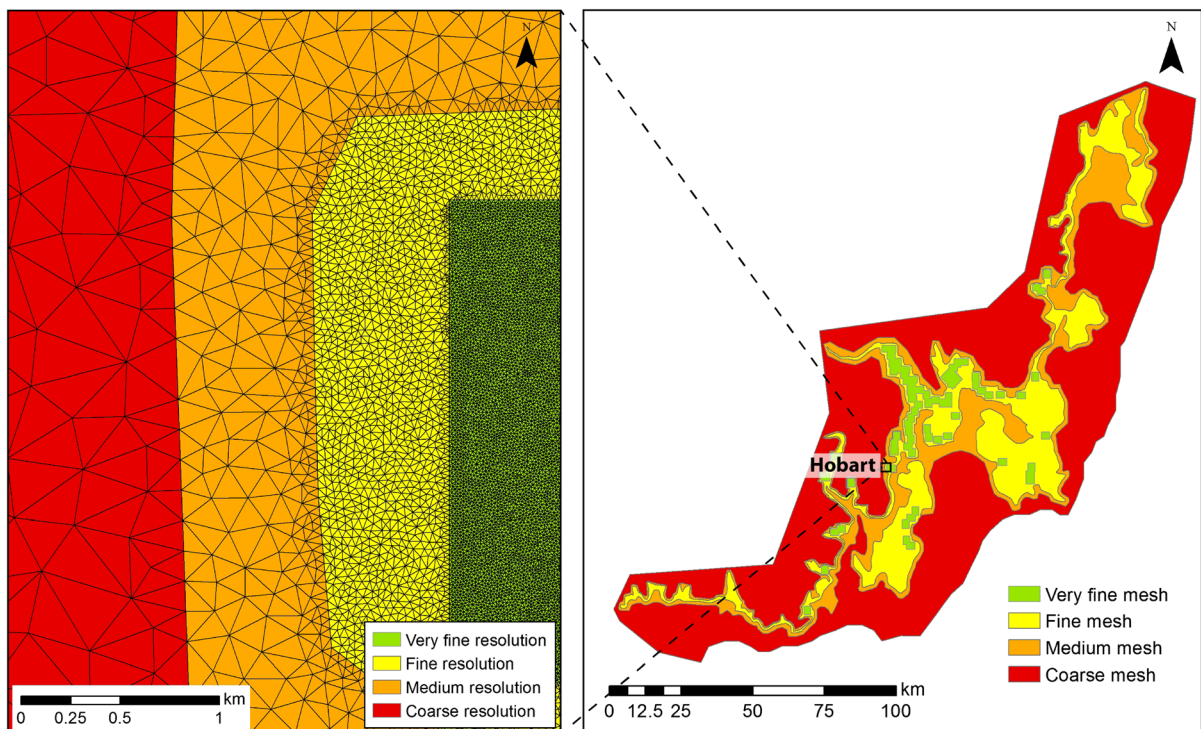


Figure 3

Details of mesh resolution zones across the study area

Table 2

Data sources used to construct the elevation model

Data source	Type	Year obtained	References
TasPorts bathymetry	Swath bathymetry	2010–2013	Unpublished
SeaMap: Bruny Bioregion Dataset	Sonar point data (Bathymetry)	2001	Barrett et al. (2001)
SeaMap: Derwent Estuary Programme	Sonar point data (Bathymetry)	2007	Lucieer et al. (2007)
SeaMap: Pittwater Estuary	Sonar point data (Bathymetry)	2002	Davies et al. (2002)
AusENC (Australian Hydrographic Office)	Depth soundings (Bathymetry)	Up to 2015	Licensed data
Private kayak soundings: Huon River	Depth soundings (Bathymetry)	Unknown	Unpublished
Australian Bathymetry and Topography Grid	National gridded bathymetry model (200 m resolution)	2009	Whiteway (2009)
Terrestrial LiDAR surveys:		2011–2015	Geoscience Australia, National
Coal Mines (Tasman Peninsula) 2015			Elevation Data
DPAC Coastal 2014			Framework
Geoscience Australia, Greater Hobart 2013			(NEDF)
Mt Wellington, 2011			DPIPWE (2007)
Tas DEM 25 m	Photogrammetric (topographic) contours		

Table 3

Manning's n coefficients of roughness applied in the model, as assigned by surface type

Mannings n	Surface type
0.5	Solid buildings
0.071	Built-up areas
0.055	Vegetated areas
0.035	Land (default)
0.03	Bare ground
0.025	Water courses
0.018	Roads
0.01	Oceans and estuaries

resulting from the 2004 Indian Ocean tsunami was modelled by Jakeman et al. (2010) using ANUGA, and good agreement was obtained between modelled data and measured inundation extents, flow depths and velocities.

ANUGA uses a finite volume modelling method for solving shallow water wave equations and the DE0 flow algorithm was used in this study. The tsunami modelling scripts were built in Python 2.7 and major processing was performed through cloud hosted computing on Amazon Web Service. The processing time for the longest model run (maritime hazard scenario; a 13 h simulation) was approximately 80 h.

The initial water level was set at highest astronomical tide, to represent a worst case scenario of tsunami and tidal interaction. An assumed value of 0.8 m AHD was applied across the entire domain, which represents an average across the region (range 0.70–0.86 m AHD).

2.2.1 Development of the Dune Erosion Operator

In undertaking the initial coastal inundation modelling, it became clear that there were several locations where sand dunes were providing some level of protection for property or assets behind the dune line. Hobart Airport is one such location. To better understand and quantify the protection provided by these dunes, an operator script was developed in Python and incorporated into the model scripts for Scenario C (Rigby et al. 2017).

The purpose of this operator was to quantify the increase in risk from a tsunami scouring out a protective dune line, and so focuses on the erosion process rather than the subsequent transport and deposition process. The erosion mechanism is based on the work of Froelich (2002) and assumes a clear water scour with no significant sediment entrained in the approaching wave that could impact detachment rates. At each time step, the operator firstly simulates the detachment of sand by water flowing over the surface, by calculating the bed stress for each mesh

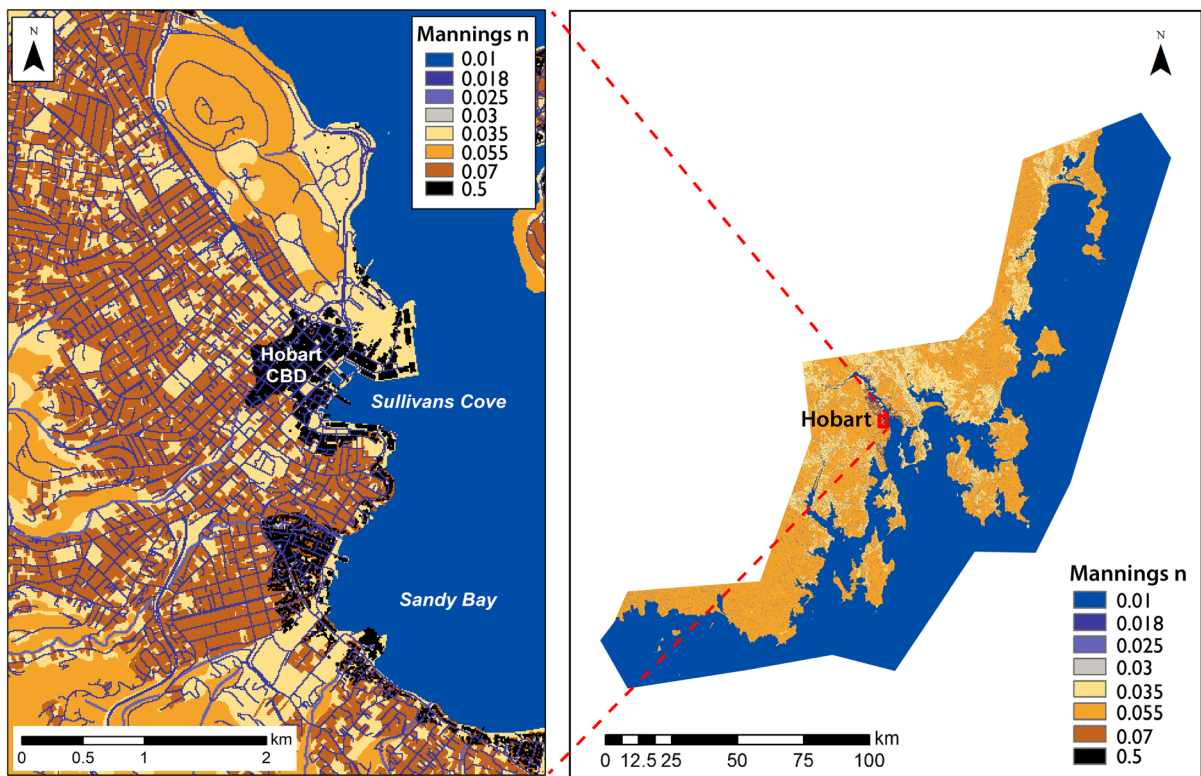


Figure 4
Manning's *n* zones as applied across the model domain

centroid (Eq. 1) and comparing this value with the detachment rate (the critical bed shear stress T_{crit} as per Froelich 2002; Eq. 2). The operator then simulates the collapse, fluidisation and removal of sand as a consequence of the erosion process creating face slopes that would be steeper than their angle of repose. Each triangle within the erosion zone is checked against neighbouring triangles with the aim of creating a stable surface that does not drop below a specified base level (1–3 m AHD depending on location). Further details of the development and testing of this operator script are provided by Rigby et al. (2017):

$$T_{bed} = \frac{Wd * g * n^2 * m^2}{d^{2.333}} \quad (1)$$

$$S_k = \frac{Kd * (T_{bed} - T_{crit})}{Sd} \quad (2)$$

where: Wd = water mass density (1000 kg m^3),
 g = acceleration due to gravity (9.8 ms^{-2}),

n = Manning's *n* (sand $n = 0.025$), m = absolute momentum ($(mx^2 + my^2)^{0.5}$), d = water depth (ANUGA stage-elevation), Kd = the detachment rate ($0.0250 \text{ kg s}^{-1} \text{ m}^{-2} \text{ Pa}^{-1}$), Sd = sediment mass density (1800 kg^{-3} for packed siliceous sand).

The primary objective of Scenario C was to explore the level of protection afforded by the present (2015) Seven Mile Beach dune line, which separates Hobart Airport from the waters of Frederick Henry Bay. However, the opportunity was also taken to investigate the possible loss of protection at twelve other sites that are potentially prone to erosion (Fig. 5).

2.3. Data Processing

Raster and time series outputs were extracted from the netcdf model files and analysed to map maximum flow depths and maximum velocity.

CSV files of time series data for water level and velocity were extracted at 187 point locations near

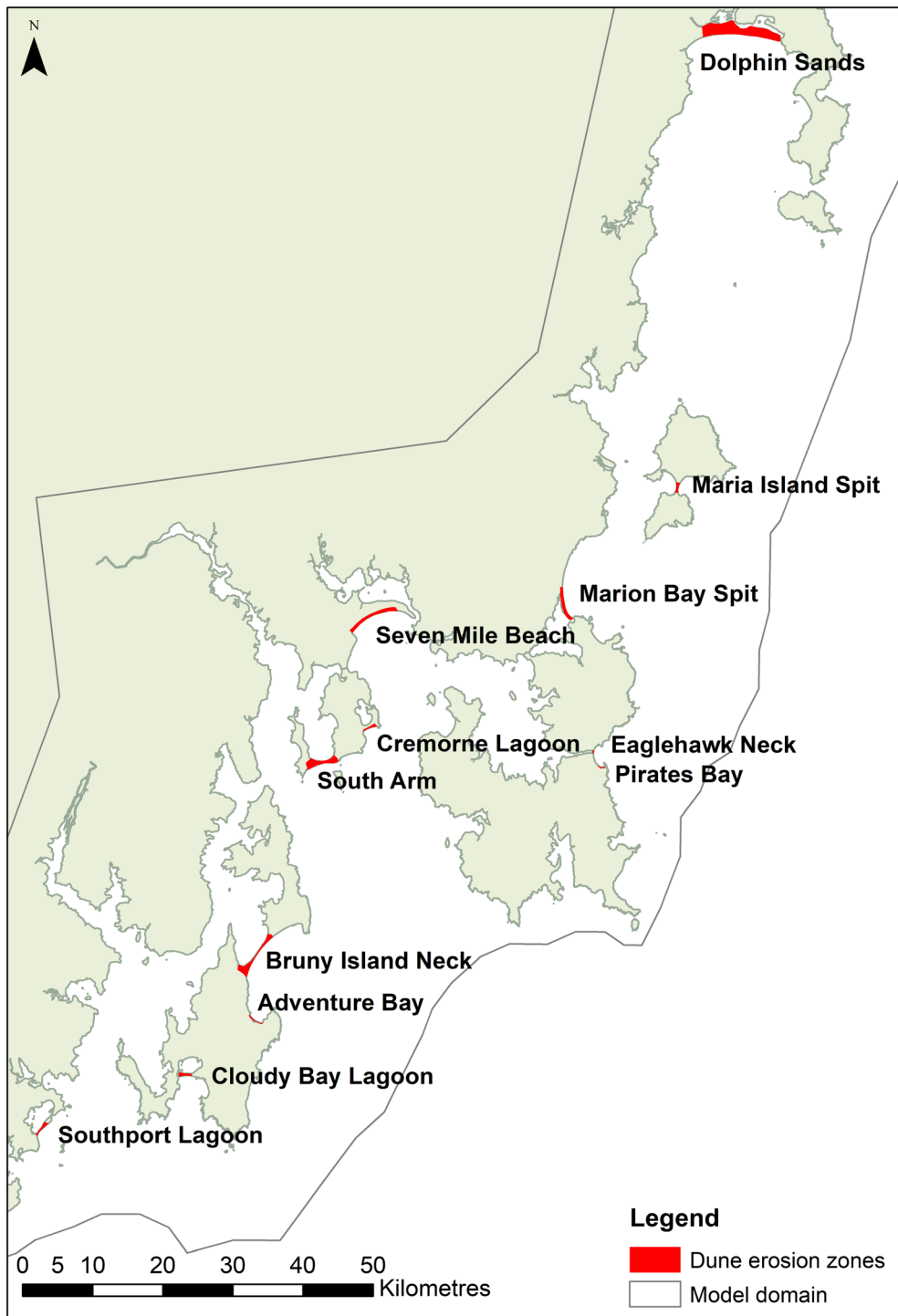


Figure 5
Location of the areas modelled with the active dune erosion operator

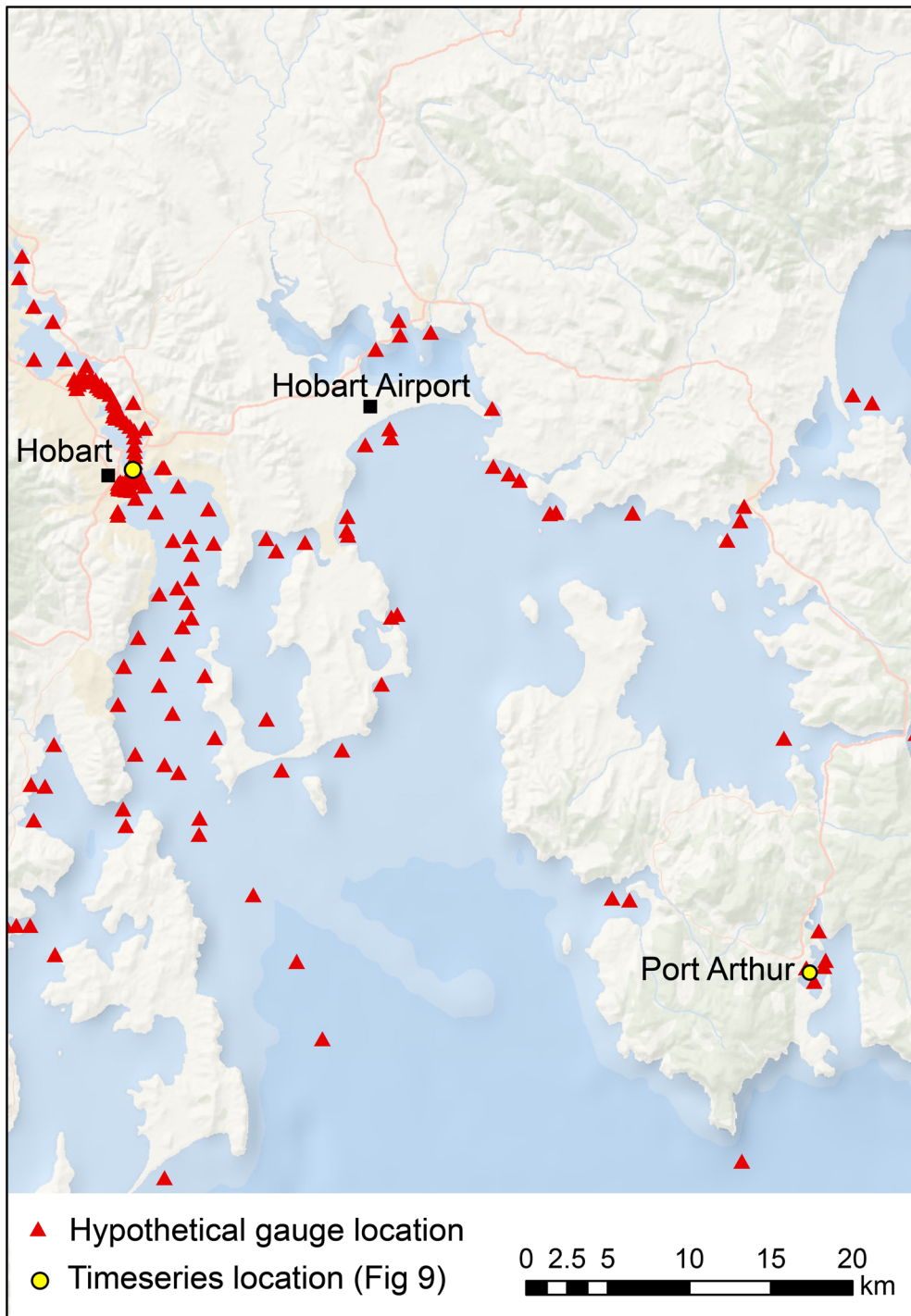


Figure 6
Gauge locations for the maritime hazard scenario

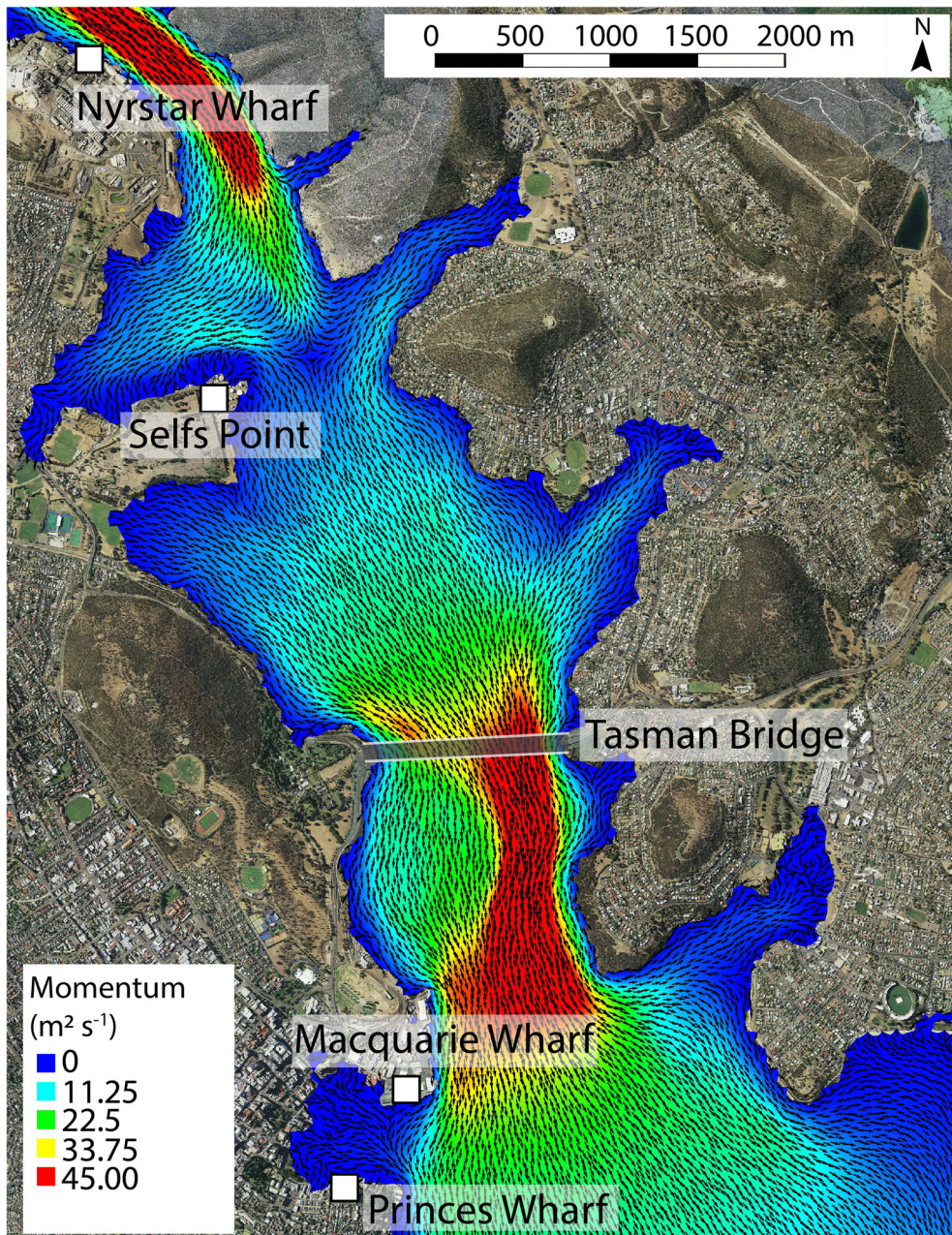


Figure 7

Snapshot of simulated tsunami momentum in the Derwent Estuary near Hobart city. Locations of port and dock areas mentioned in the maritime hazard results are also shown

coastal communities or where maritime hazard may be significant, such as shipping lanes, marinas and embayments (Fig. 6). The following parameters were calculated from the time series for the maritime hazard assessment: tsunami arrival time (arrival of

the first peak post-earthquake, with a threshold of 0.1 m), maximum wave height (wave crest—trough), time of maximum wave height, period, average wavelength of the first two waves, maximum current speed, maximum celerity (wave speed), maximum

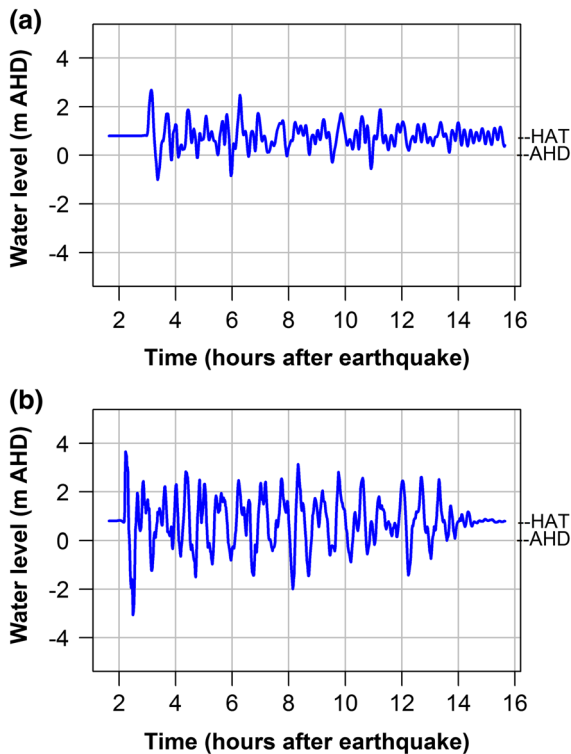


Figure 8

a Tsunami time series plot for the primary shipping channel near Tasman Bridge. **b** Tsunami time series plot for Port Arthur

possible instantaneous speed (current speed + celerity), maximum water level (m AHD), minimum water level (m AHD) and turbulence ratio (wave height: water depth). Note that wave heights are used for the maritime hazard analysis, rather than wave amplitudes, as the total variation from peak to trough is important for assessing shipping hazard and berthing requirements.

The final outputs include video animations of the modelled tsunami and a series of maps depicting maximum possible impacts around 71 coastal communities, which show coastal inundation, maximum offshore current speed and potentially turbulent areas (Kain et al. 2018).

2.4. Field Validation

Site visits were undertaken in order to visually assess the inundation extents at important sites or areas where modelled impacts were significant. Sites were photographed and key infrastructure at risk of

flooding was identified. In some cases, features were identified that may increase or mitigate the mapped risk; for example, subsurface drains could allow greater tsunami penetration, whereas dense vegetation may limit it.

3. Results

The geometry of the subduction zone and rupture scenario is such that the wave would arrive as a leading peak (rising water level), rather than a trough (receding water). The modelled tsunami wavelengths are in the order of 500 m nearshore (increasing to > 5 km offshore) and, consequently, the tsunami manifests as a gradual rise and fall in water level that occurs over a period of 10–20 min. Significant seiche and wave reflections are predicted in the channel and embayments, and these would generate considerable water disturbance and localised amplification. The first tsunami wave would reach the exposed east coast approximately 2 h and 10 min post-earthquake, and around 3 h in the Hobart CBD area. A snapshot of the simulated momentum in the Derwent Estuary is given in Fig. 7.

3.1. Maritime Hazard Analysis

Within the principal shipping channel, modelled wave heights vary from 2.4 m at the southern end (Fig. 8a) to 5.1 m off Newtown Bay, with many values falling between 3.5 and 4.5 m. Maximum modelled wave speed falls between 8.0 ms^{-1} (mid channel at the entrance to Prince of Wales Bay) and 16.8 ms^{-1} . Maximum induced current speeds are in the order of $1.0\text{--}3.6 \text{ ms}^{-1}$ and severe turbulence would not be expected in the shipping channel, as the water there is deep relative to the wave height.

The tsunami impacts would be variable in the port and dock areas. Maximum predicted wave heights range from 2.7 to 5.0 m and maximum simulated celerity varies between 2.5 and 15.9 ms^{-1} . In general, predicted wave speeds are $< 5.1 \text{ ms}^{-1}$ within the dock areas and along the shore, but higher values occur further out in the channel. Turbulence would be expected in most port and dock areas, with Prince of Wales Bay, Macquarie Wharf and Princes



Figure 9

Locations of the berths at Macquarie Wharf and Princes Wharf

Wharf particularly affected. A backup of water is observed in places, most notably at Constitution Dock near Hobart CBD (Fig. 9). Following inundation by the first wave in the model, the water does not fully drain from the area before the arrival of the second wave and the water level remains at least 1.5 m higher than the starting level for the duration of the model run. However, at no point does the water height exceed that of the first wave peak level.

Potential consequences include damage to boats and infrastructure from collisions, breakage of moorings due to water level or currents, spills and pollution, and foundering or sinking of smaller craft. A summary of berth information and modelled tsunami wave parameters is given in Table 4. Because most of the commercial shipping around Hobart port have drafts greater than the inundation levels, there is little likelihood of these ships being

lifted onto the berth. However, smaller vessels/craft with shallower drafts, e.g. less than 1.2 m at the CSIRO Wharf (Princes Wharf 4; Fig. 9), are at risk of being lifted on to the berth deck. There is also a significant risk of vessels breaking adrift if moorings are not tended to deal with the rising and falling levels. This could cause major damage to the drifting ship, other vessels and infrastructure.

For vessels and small craft underway at the time of the tsunami, loss of nav aids and steering capacity due to the tsunami wave(s) and induced currents is expected. These issues could then lead to collisions and would be a particular concern for large ships around the Tasman Bridge (Fig. 1). The maximum modelled wave height in the main navigational channel at the bridge is 5.1 m, with a simulated maximum current speed of 2.5 ms^{-1} . Given that the channel is 100 m wide with clearance of 44 m and a maximum permitted vessel passage of 185 m (in length), consequences could be catastrophic.

Modelled tsunami arrival times range from 2.5 to 3.25 h post-earthquake, with a difference of 36 min between the outer limit of the shipping channel (off Iron Pot, to the anchorages at Prince of Wales Bay (Fig. 1). A timeline based on the modelled event and the Tasmanian State Tsunami Emergency Response Plan, is given in Table 5.

Given an evacuation warning time window of 1 h and sufficient crew, pilot boat availability and standby engine power, it may be possible for some large ships to evacuate from Hobart port and Nyrstar/Risdon wharves. However, the required passage through Tasman Bridge limits the feasibility of evacuation. The decision to evacuate to deeper water depends heavily on the ship's mobilisation status as well as distance to deeper water, and in many cases it may be safer to remain in port and evacuate crew to higher ground. Specific mobilisation and evacuation times have been calculated for vessels that frequent the Hobart port areas (Table 6). For smaller craft, the primary advice is to secure the craft and evacuate the crew to higher ground. Significant water disturbance and turbulence is expected at all marinas and anchorages around Hobart, making small craft manoeuvrability difficult and/or unsafe.

Table 4

Summary of berth data alongside modelled tsunami wave heights and induced current speeds for each locality (locations shown in Figs. 1, 7 and 9)

Location or berth	Declared depth (metres)	Height of berth above chart datum (metres)	Number of bollards	Usage	Tsunami arrival time (post earthquake)	Max wave height (m)	Inundation height above berth deck (m)	Induced current speed (ms^{-1})
Main navigational channel off Iron Pot	14.1 m (Iron Pot Bar)	–	–	Shipping channel	2 h 30 m	4.7	–	1.8
Main navigational channel, Tasman Bridge		–	–	Shipping channel	3 h	5.1	–	2.5
Main navigational channel off Newtown Bay				Shipping channel	3 h 10	5.1	–	3.2
Princes Wharf 1	7.3	3.31	13	Antarctic Supply, Small	3 h	3.4	0	0.3
Princes Wharf 2-3	9.0	3.25	8	Cruise, Naval	3 h	3.1	0	0.5
Princes Wharf 4	7.2	2.79		CSIRO	3 h	3.6	0	0.6
Macquarie 1	4.1	3.1 to 4.01		Small Fishing, Fish Unloading Facility	3 h	3.1	1.0	0.4
Macquarie 2	9.1	4.01	10	Larger Fishing, Caustic Acid	3 h	3.8	1.0	0.6
Macquarie 3	9.9	4.01	12	Car Carriers, Bulk Products, Cruise, Antarctic	3 h	3.5	1.0	0.7
Macquarie 4-5	13.0	4.01-2.79	15	Container Traffic, Break Bulk, Cruise, Antarctic	3 h	3.2	1.0	0.8
Macquarie 6	11.4	2.79-3.2	13	Lay-up berth	3 h	3.3	1.0	1.0
Self's Point	14.4	3.71	10 on wharf; 4 on	dolphins	Fuel Terminal, Bunkering Facility	3 h 10 m	4.9-5.0	0.5
2.1-2.4 Risdon (Nyrstar)	10.2	3.33	19	Concentrates, Acid, Fertiliser	3 h 10 m	2.7-4.5	~ 0.1	2.6-2.8

A map of berth sites at Princes and Macquarie Wharves is provided in Fig. 9

3.2. Coastal Hazard and Inundation

This section is concerned primarily with results from Scenario B (as outlined in Sect. 2). Simulated coastal inundation is generally greatest in exposed eastern areas or where river channels act as a conduit for inland penetration. A funnelling of the tsunami energy is observed in the simulation as it passes through the narrow channel northwest of the Tasman

Bridge, which may also be exacerbated by wave reflection from the steep bathymetry on the eastern shore.

Modelled flooding around the central Hobart waterfront (Fig. 10) extends up to 100 m inland in places, but depths are no more than 1 m with a maximum run-up elevation of 2.5 m AHD. The results indicate that the wharf areas and surrounding car parks would be inundated, and the buildings along

Table 5

Timeline of tsunami arrival and predicted warning times

Warnings and wave arrival summary (approximations)	
Event	Elapsed time
Earthquake occurrence	0
National Tsunami watch alert	30 min
Specific watches and warnings issued	1 h
Tasmania Police issue additional warnings	
Realistic notification of Hobart public	2 h
Wave reaches Tasmania	2 h
Wave reaches Iron Pot	2 h 35 min
Wave reaches Sullivans Cove	3 h
Wave reaches Selfs Point	3 h 05 min
Wave reaches Risdon (Nyrstar)	3 h 08 min
Wave reaches Prince of Wales Bay	3 h 10 min

Tsunami watch and warning estimates derived from the Tasmanian State Tsunami Response Plan

the waterfront would most likely be affected with potentially significant impacts for underground infrastructure. Modelling results also suggest that the tsunami would be funnelled into the narrow embayments on both sides of the Derwent Estuary, causing flooding at the head of these bays and impacting the nearshore marinas and recreational areas.

The most heavily affected areas are Tasman Peninsula and Bruny Island (Fig. 1), with flow depths predicted to reach > 4 m with an inundation limit of several hundred metres inland in many locations. Significant inundation is predicted at Port Arthur,

Nubeena and Adventure Bay, with simulated flooding reaching several hundred metres inland and a maximum flow depth of 5 m near the coast. A time series graph for Port Arthur is given in Fig. 8b.

In particular, simulated water levels at Eaglehawk Neck reach 14 m AHD and severe flooding could occur through dune breaching and overtopping. This extreme modelled water level arises from the interaction of the tsunami wave with the shape of Pirates Bay in the simulation. We suggest this water level not be taken at face value, as the reality would vary with a small change in wave characteristics, timing or approach direction at this location. In this simulation, a combination of wave refraction from the neighbouring bay and wave reflection from the semi-circular embayment results in the formation of large vortices at each end of the embayment, along with constructive wave interference and focusing that together cause a simulated wave amplitude of 14 m. Notably, the actual incoming wave crest elevation (prior to the amplification) is approximately 7 m, which is in line with other exposed coastal locations.

Regardless of any occurrence of tsunami amplification, the impact would remain severe. Any significant pre-existing low point in east-facing dunes would still be exploited as a conduit by an incoming tsunami of 7 m. This level would result in several state highways becoming compromised, which would isolate communities beyond the choke points of Eaglehawk Neck and Bruny Neck, and some coastal locations north of Tasman Peninsula.

Table 6

Estimated time to mobilise and evacuate to deeper water for ships that frequent Hobart Port

Estimated time to reach				Distance to White Rock Pt (km)	Distance to open ocean (km)
Location	Vessel type	Open ocean*	Deep water in shipping channel**		
Nyrstar Wharf	Bulk carrier	2 h 35 m	1 h 20 m	17.6	45.4
Selfs Point Wharf	Oil tanker	2 h 25 m	1 h 25 m	15.7	43.5
Princes Wharf	Research vessel	1 h 50 m	55 m	12.0	39.8
Macquarie Wharf	Cruise ship	1 h 35 m	50 m	12.0	39.8

*45 m depth, Storm Bay; **33 m depth, White Rock Pt

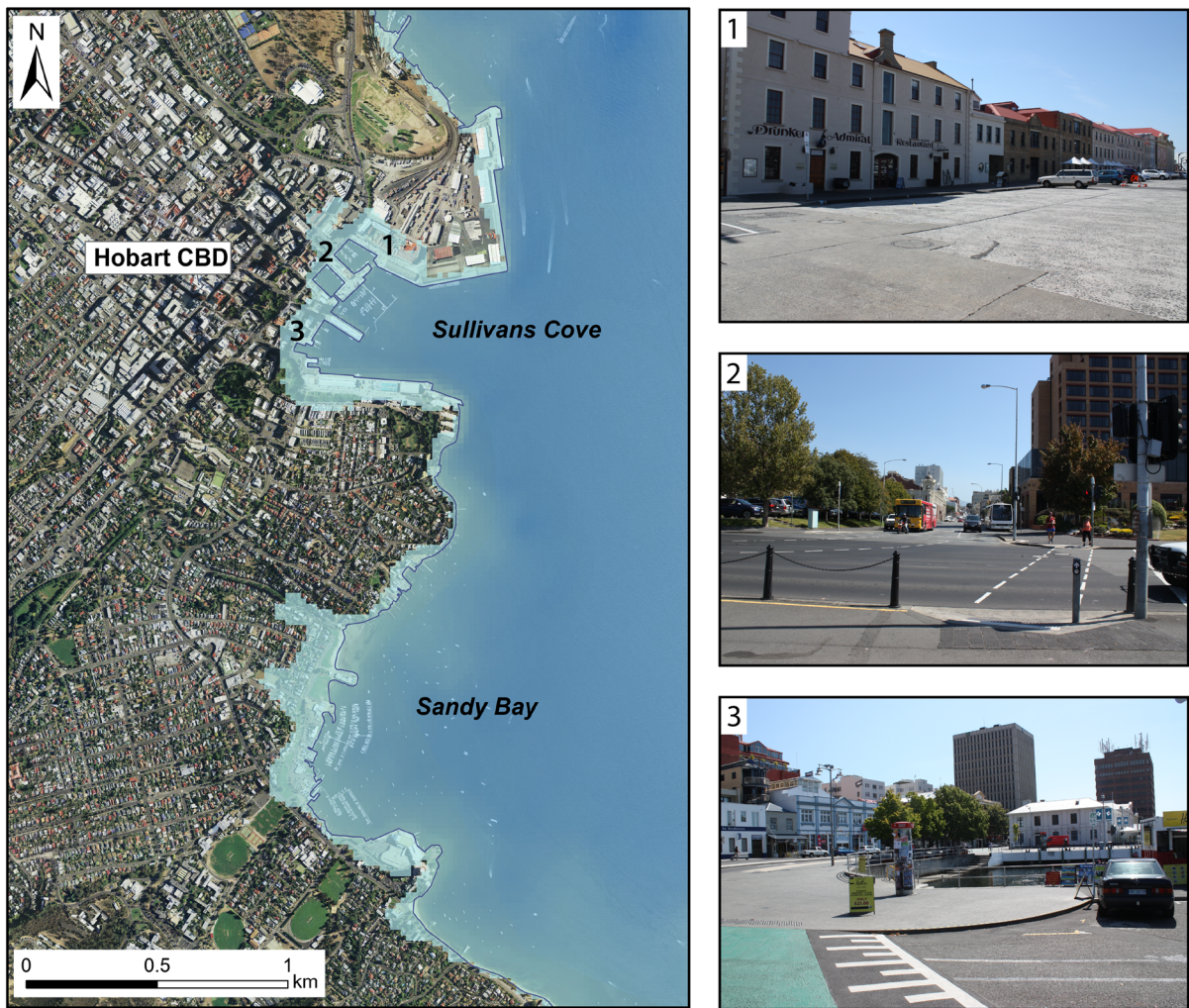


Figure 10

Modelled inundation in Hobart CBD and Sandy Bay, accompanied by field validation photos showing areas of predicted flooding around the city waterfront

Predicted inundation is less severe at Hobart city waterfront and in the bays inland from the CBD. However, significant flooding is predicted in Kingston and flooding via the Newtown Rivulet would compromise highway access between Moonah and Newtown (Fig. 1).

3.3. Dune Erosion and Risk to Hobart Airport

This section presents results from Scenario C (see Sect. 2). Modelling results show that the wave height would be significantly reduced as the tsunami travels

through Frederick Henry Bay (Fig. 11). As such, the dune line (as present in 2016) is sufficient to protect the airport runway and infrastructure from inundation for the modelled event. Little dune erosion was apparent in the simulation at Seven Mile Beach, although this could change if the dune structure altered (for example, through a blowout or removal of part of the dune). It is also important to note that part of the dune line is only marginally higher than the approaching wave amplitude, so a relatively minor reduction in dune height could create significant local breaches. The dune line in front of the runway is well

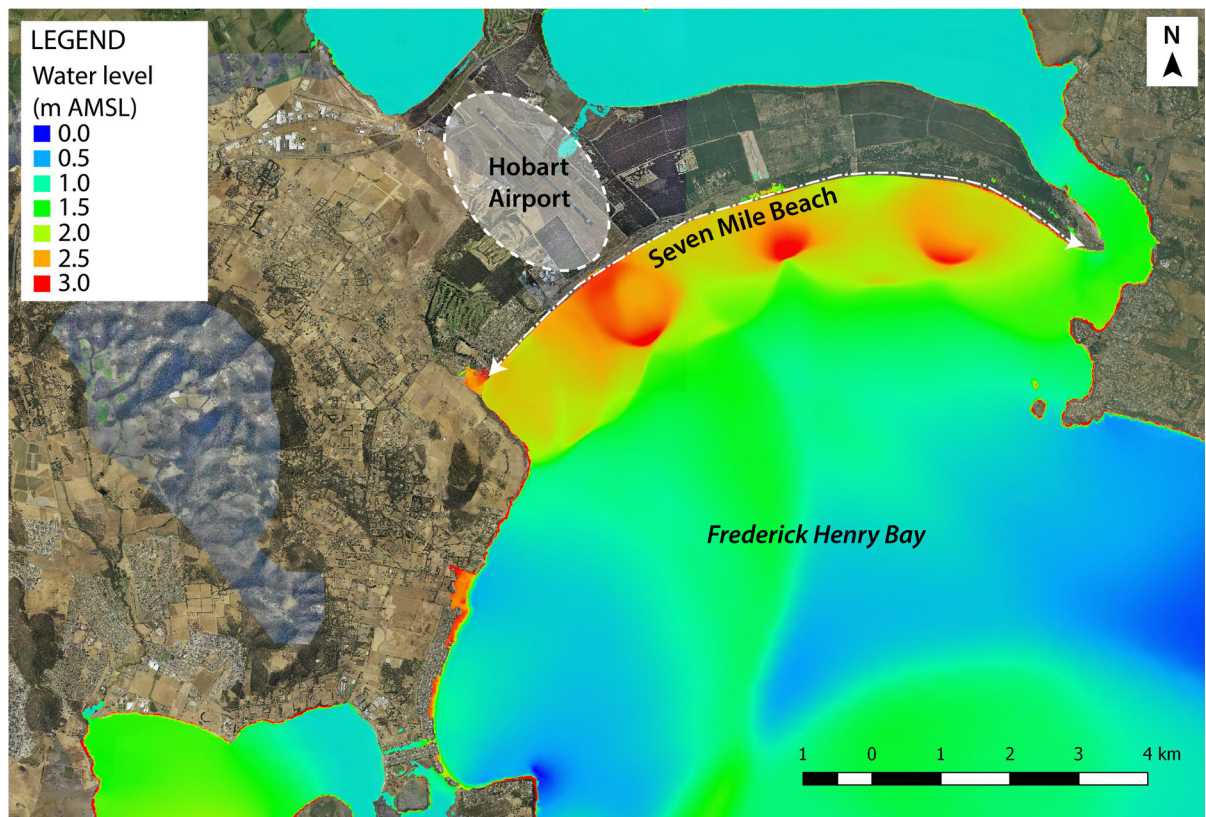


Figure 11

Snapshot of the modelled wave as it reaches Seven Mile Beach in front of Hobart Airport. The dune line is sufficiently high that the wave is largely reflected back from the beach (red pattern, nearshore) and does not penetrate the dunes in front of the runway

developed, but if it were to be removed, an incoming tsunami wave would likely breach the barrier at this location.

In addition to the detailed modelling of the airport site, the opportunity was taken to investigate the possible loss of dune protection at other erosion prone sites in southeast Tasmania. Erosion-enabled modelling suggests that significant erosion and inundation could potentially affect infrastructure and/or settlements at the following sites: Eaglehawk Neck, Bruny Island Neck, Adventure Bay Beach, South Arm Neck and Pirates Bay Beach (Fig. 5). A detailed analysis of the impact of the erosion operator was performed at Bruny Neck, where approximately 900,000 m³ of sand was removed during the simulation. As shown in Fig. 12a, up to 2.5 m of sand was eroded in places. A comparison of modelled tsunami flow depths with and without the erosion operator showed a water level

increase of 3 m where the eroded dunes allowed greater tsunami penetration (Fig. 12b). Conversely, the comparison showed a decrease in maximum stage immediately seaward of the eroded dune line, as a consequence of reduced wave reflection.

4. Discussion

Modelling is an excellent tool for estimating the impacts of a tsunami event, but some inherent limitations must be recognised. Firstly, ANUGA is a 2D model library, which means that vertical motion cannot be resolved in the simulation. As such, factors such as wave breaking and turbulence are not directly simulated.

The tidal level was set to HAT at the beginning of the simulation and the subsequent water level and

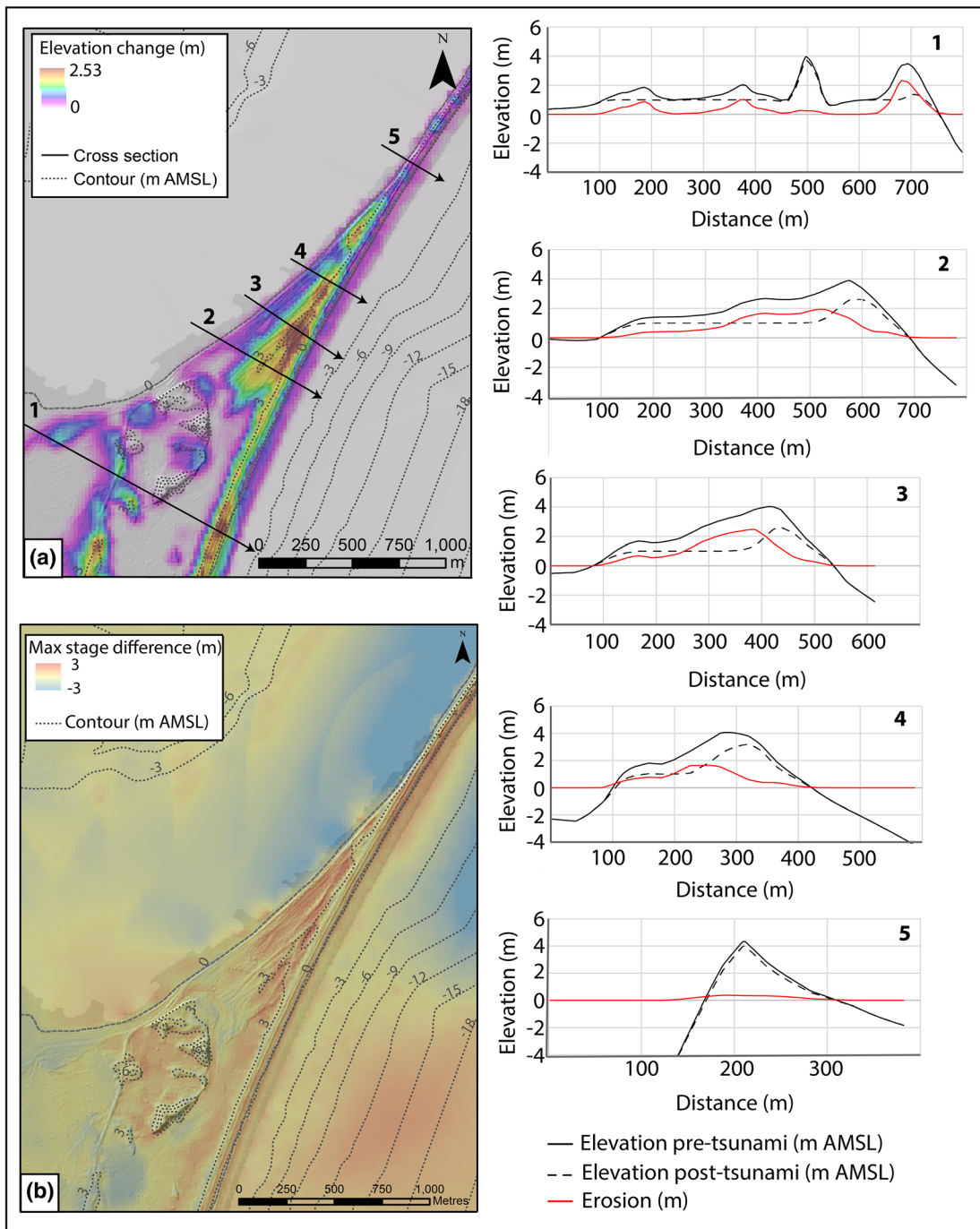


Figure 12

Comparison of the effects of the dune erosion operator at Bruny Neck. **a** Map of erosion patterns across the study area, with the location of cross section profiles 1–5. Plots of the pre and post-tsunami elevation along these profiles are presented to the right of the figure. **b** Map showing the difference in maximum stage when comparing model runs with and without the dune erosion operator enabled

current fluctuations do not account for ongoing tidal variation and currents. The interaction of the tsunami with tidal fluctuations was not feasible given the model size and computational constraints. However, the sensitivity of the modelled inundation to tidal phasing is an interesting avenue for further work. Additionally, it would be beneficial to model historical events and compare the results with tide gauge observations, in order to better understand and quantify the uncertainties within our model data.

Onshore tsunami flooding is controlled by coastal geometry, erosion and land use/cover. The event was modelled based on elevation data from a snapshot in time, so changes in dune form or land cover would influence actual tsunami behaviour. Every effort was made to accurately model the effects of vegetation and building cover through the Manning's roughness model input, but this is again a best approximation of reality. Similarly, it is important to note that the parameters used in the dune erosion operator do not distinguish between bare sand and dunes that are vegetated with grass and/or trees. We recommend that further work be done to test the variation in detachment rates for bare and stabilised dunes.

The resolution of the mesh with respect to topographic changes has caused anomalous run-up values in areas of steep relief. Because the mesh represents a modelled surface generated from an elevation model, it does not properly represent vertical or near-vertical surfaces such as coastal cliffs and artificial structures like wharf edges. It is possible to use break lines in ANUGA to account for buildings and vertical features, but due to the large spatial extent and complexity of our model this was not attempted. As a consequence, the maps may occasionally show flow depths that appear extreme (e.g. 10 m along the cliffs at Lindisfarne). The higher the mesh resolution, the less this problem occurs, as the closer the modelled surface reflects reality. These anomalies are relatively easy to identify in the maps and have little effect on the interpretation of the inundation extent.

These results do not constitute a tsunami risk assessment. This would require consideration of a variety of tsunami sources with a range of magnitudes and return periods. However, an analysis of vulnerable places, properties and infrastructure should be undertaken alongside a review of Southeast

Tasmania's tsunami emergency response plan(s) based on this 'worst case scenario' of a large tsunami with relatively little warning time.

Further work is underway to perform tsunami modelling for other parts of Tasmania, using the PTHA 2018 (Davies and Griffin 2018). A comparison of the two PTHA databases (2008 versus 2018) is described by Davies and Griffin (2018) and the authors report that the higher magnitude scenarios behave similarly despite some significant differences in methodology between the two assessments. As such, we are confident that the results obtained in this study using the PTHA 2008 remain valid; however, it would be useful to re-run the inundation model using input data from the PTHA 2018 in order to ensure a consistent methodology across Tasmania.

To complement the modelling work and understand past tsunamis that have affected Tasmania, work is underway to search for geological palaeo-tsunami evidence in exposed eastern locations. Previous work has recognised the scope for palaeo-tsunami studies in Tasmania (e.g. Morris and Mazengarb 2009; Sharples 2006) and a previous palaeo-tsunami site has been studied at Bruny Island (Clark et al. 2011), but further work is needed to connect this evidence with a wider event and compare modelled inundation distances and flooding locations with sedimentary tsunami evidence.

5. Conclusions

Modelling results suggest that Southeast Tasmania could be significantly affected by a maximum credible tsunami event, resulting from a Mw 8.7 rupture of the Puysegur subduction zone. The work presented here builds upon initial inundation modelling performed by Geoscience Australia in 2009, by incorporating new high-resolution elevation data and addressing specific questions related to maritime hazard and risk to Hobart Airport. This approach allows a "whole-coast" hazard assessment for the region and highlights the differences in tsunami timing and coastal interactions across the entire area.

Tsunami arrival times range from approximately 2 h at the eastern coast, to 3 h at Hobart wharves. Significant water disturbance in the form of currents,

extreme water level changes and turbulence is predicted in all coastal and nearshore environments, but does not generally extend to the main shipping channel in the Derwent estuary. Such disturbance would cause considerable risk to marine craft and could result in ships breaking adrift, damage to boats and infrastructure, and pollution. The maritime hazard assessment suggests that the feasibility of evacuation to deeper water is questionable, given the short timeframes involved, and securing/tending of vessels and evacuation of crew to land is generally recommended.

The simulations predict severe inundation levels (> 4 m flow depth) in exposed coastal communities on the east coast. Significant inundation (> 3 m flow depth) is predicted in the embayments along both shores of the Derwent estuary, including the Hobart city waterfront and wharves. The potential for dune erosion was included in the modelling for Hobart Airport, and results suggest that the current dune line would not be breached or overtopped by a tsunami of this magnitude at this location. However, inundation could occur if the dune was to be substantially lowered or partially removed in the future.

These results could be useful for an analysis of vulnerable communities and infrastructure for the case of a maximum credible tsunami, and feed into regional hazard management planning. In addition, palaeotsunami studies would help validate the modelling results and provide useful information regarding inundation extents and recurrence intervals of tsunamis that have previously affected Tasmania.

Acknowledgements

This project was funded by a grant from the Natural Disaster Resilience Grants Programme (NDRGP), in conjunction with Mineral Resources Tasmania. Assistance with ANUGA troubleshooting was kindly provided by Stephen Roberts of ANU. Claire Kain and Colin Mazengarb publish with permission of the Director of Mines, Tasmania.

Publisher's Note Springer Nature remains neutral with regard to jurisdictional claims in published maps and institutional affiliations.

REFERENCES

- Australian Bureau of Statistics. (2018). Regional Population Growth, Australia, 2017–2018. <https://www.abs.gov.au/AUSSTATS/abs@.nsf/mf/3218.0>. Accessed 23 Aug 2019.
- Baldock, T. E., Barnes, M. P., Guard, P. A., Hie, T., Hanslow, D., Ranasinghe, R., Gray, D., & Nielsen, O. (2007). Modelling tsunami inundation on coastlines with characteristic form. In: Proceedings of the 16th Australasian Fluid Mechanics Conference: Gold Coast, Australia, pp. 939–942.
- Barrett, N., Sanderson, J. C., Lawler, M., Halley, V., & Jordan, A. (2001). Mapping of inshore marine habitats in south-eastern Tasmania for marine protected area planning and marine management. Tasmanian Aquaculture and Fisheries Institute Technical Report Series 7.
- Beccari, B. (2009). Measurements and impacts of the Chilean tsunami of May 1960 in New South Wales, Australia. New South Wales State Emergency Service Report 05/0576, p 42.
- Borrero, J. C., Lynett, P. J., & Kalligeris, N. (2015). Tsunami currents in ports. *Philosophical Transactions of the Royal Society A*. <https://doi.org/10.1098/rsta.2014.0372>.
- Bricker, J. D., Gibson, S., Takagi, H., & Imamura, F. (2015). On the need for larger Manning's roughness coefficients in depth-integrated tsunami inundation models. *Coastal Engineering Journal*. <https://doi.org/10.1142/s0578563415500059>.
- Burbidge, D., Mleczko, R., Thomas, C., Cummins, P., Nielsen, O., & Dhu, T. (2008). A probabilistic tsunami hazard assessment for Australia. Geoscience Australia Professional Opinion 2008/04, Canberra.
- Chow, V. T. (1959). *Open-channel hydraulics*. New York: McGraw-Hill Book Company.
- Clark, K., Cochran, U., & Mazengarb, C. (2011). Holocene coastal evolution and evidence for paleotsunami from a tectonically stable region, Tasmania, Australia. *The Holocene*, 21, 883–895.
- Commonwealth of Australia—Geoscience Australia. (2016). ARR: australian rainfall and runoff; a guide to flood estimation. <http://arr.ga.gov.au/arr-guideline>. Accessed 11 Dec 2016.
- Cox, D. C., & Mink, J. F. (1963). The tsunami of 23 May 1960 in the Hawaiian Islands. *Bulletin of the Seismological Society of America*, 53, 1191–1209.
- Davies, P. E., Crawford, C. M., Wells, F. A., Dunstan, P., & Mitchell, I. M. (2002). Environmental flow assessment of the lower coal river and pitt water estuary. Report to DPIPWE from Freshwater Systems and the Tasmanian Aquaculture and Fisheries Institute. p. 203.
- Davies, G., & Griffin, J. (2018). The 2018 Australian probabilistic tsunami hazard assessment: hazard from earthquake generated tsunamis. Geoscience Australia, Record 2018/41. <https://doi.org/10.11636/Record.2018.041>
- Department of Primary Industries, Parks, Water and Environment (DPIPWE). (2007). LIST Tasmania 25 metre Digital Elevation Model. http://listdata.thelist.tas.gov.au/opendata/index.html#LIST_Tasmania_25_Metre_Digital_Elevation_Model. Accessed 1 Aug 2016
- Department of Primary Industries, Parks, Water and Environment (DPIPWE). (2013). TASVEG 3.0: Tasmanian vegetation monitoring and mapping program. Resource Management and Conservation Division
- Fernandes, M. A. G. (2009). Systematic comparison on the inundation response of AnuGA and COMCOT tsunami modelling

- codes applied to the Boca do Rio and Alvor Bay area. Unpublished PhD Thesis, Universidade do Algarve. p. 75.
- Froelich, D. (2002). IMPACT project field tests 1 and 2 “Blind” simulation. 2nd IMPACT Project Workshop, Mo-i-Rana Norway.
- Goff, J., & Chagué-Goff, C. (2014). The Australian tsunami database: a review. *Progress in Physical Geography*, 38, 218–240.
- Hasan, H., Lodhi, H. A., LeVeque, R. J., Lodi, S. H., & Ahmed, S. (2017). Assessing tsunami risk for Karachi Port through simulation of currents that were reportedly produced there by the 1945 Makran tsunami. In: Proceedings of the 16th World Conference on Earthquake, Santiago Chile, January 2017
- Heath, R. A. (1976). The response of several New Zealand harbours to the 1960 Chilean tsunami. *Bulletin of the Royal Society of New Zealand*, 15, 71–82.
- Jakeman, J. D., Nielsen, O. M., Van Putten, K., Mleczo, R., Burbidge, D., & Horspool, N. (2010). Towards spatially distributed quantitative assessment of tsunami inundation models. *Ocean Dynamics*, 60, 1115–1138.
- Kain, C. L., Mazengarb, C., Rigby, E. H., Cohen, B., Simard, G., & Lewarn, B. (2018). Technical report on tsunami inundation modelling in South East Tasmania. Tasmanian Geological Survey Report UR2018_02. p. 160.
- Kato, Y., Suzuki, Z., Nakamura, K., Takagi, A., Emura, M., Ito, M., et al. (1961). The Chile tsunami of 1960 observed along the Sanriku coast of Japan. Report series of Tohoku University, 5. *Geophysics*, 13, 107–125.
- Land Information System Tasmania. (2016). ListData Open data. <https://listdata.thelist.tas.gov.au/opendata/>. Accessed 11 Dec 2016.
- Lucieer, V. L., Lawler, M., Morffew, M., & Pender, A. (2007). Estuarine habitat mapping in the derwent—2007. A resurvey of marine habitats by seimap tasmania. Tasmanian Aquaculture and Fisheries Institute, University of Tasmania: Hobart.
- Lynett, P. J., Borrero, J. C., Weiss, R., Son, S., Greer, D., & Renteria, W. (2012). Observations and modelling of tsunami-induced currents in ports and harbors. *Earth and Planetary Science Letters*, 327–328, 68–74.
- Lynett, P. J., Borrero, J., Son, S., Wilson, R., & Miller, K. (2014). Assessment of the tsunami-induced current hazard. *Geophysical Research Letters*, 41, 2048–2055.
- Lynett, P. J., Gately, K., Wilson, R., Montoya, L., Arcas, D., Aytore, B., et al. (2017). Inter-model analysis of tsunami-induced coastal currents. *Ocean Modelling*, 114, 14–32.
- Morris, M. K., & Mazengarb, C. (2009). Historical accounts of tsunamis in Tasmania. Tasmanian Geological Survey Record 2009/04. Department of Infrastructure, Energy and Resources, Mineral Resources Tasmania.
- Muhari, A., Charvet, I., Tsuyoshi, F., Suppasri, A., & Imamura, F. (2015). Assessment of tsunami hazards in ports and their impact on marine vessels derived from tsunami models and the observed damage data. *Natural Hazards*. <https://doi.org/10.1007/s11069-015-1772-0>.
- Mungkasi, S., & Roberts, S. G. (2013). Validation of ANUGA hydraulic model using exact solutions to shallow water wave problems. *Journal of Physics: Conference Series*, 423, 012029. <https://doi.org/10.1088/1742-6596/423/1/012029>.
- Nielsen, O., Roberts, S., Gray, D., McPherson, A., & Hitchman, A. (2005). Hydrodynamic modelling of coastal inundation. MODSIM 2005 In: International Congress on Modelling and Simulation, Modelling and Simulation Society of Australia & New Zealand, pp. 518–523.
- Okal, E. A., Fritz, H. M., Raveloson, R., Joelson, G., Pancokova, P., & Rambolamanana, G. (2006a). Madagascar field survey after the December 2004 Indian Ocean tsunami. *Earthquake Spectra*, 22, 263–283.
- Okal, E. A., Sladen, A., & Okal, E. A. S. (2006b). Rodrigues, Mauritius and Reunion islands field survey after the December 2004 Indian Ocean tsunami. *Earthquake Spectra*, 22, 241–261.
- Rigby, E., Mazengarb, C., Barthelmess, A., & Kain, C. (2017). Experiences developing and applying an ANUGA dune erosion operator to assess risk from loss of dune protection during a tsunami. In: Proceedings of the 13th Hydraulics in Water Engineering Conference. pp. 8
- Roberts, S., Nielsen, O., Gray, D., Sexton, J., & Davies, G. (2019). ANUGA user manual. Geoscience Australia. <https://anuga.anu.edu.au/>
- Sharples, C. (2006). *Indicative mapping of Tasmanian coastal vulnerability to climate change and sea-level rise: explanatory report* (p. 173). Tasmania: Consultant Report to Department of Primary Industries & Water.
- Sterzai, P., Coren, F., & Creati, N. (2015). The application of open-source software ANUGA installed on a BlueJ/Q computer for a tsunami modelling in coastal areas of city of Trieste using high resolution laser-scanning and multibeam data. *Planet-Risk*, 3(1), 121–125.
- Uslu, B., Power, W., Greenslade, D., Eblé, M., & Titov, V. (2011). The July 15, 2009 Fiordland, New Zealand Tsunami: real-time assessment. *Pure and Applied Geophysics*, 168(11), 1963–1972.
- Van Putten, K., Fountain, L., Griffin, J., Sexton, J., Nielsen, O., & Wilson, R. (2009). Capacity building for tsunami planning and preparation: inundation models for south east Tasmania. Geoscience Australia Professional Opinion. No.2009/07. Geoscience Australia: Canberra.
- Whiteway, T. (2009). *Australian bathymetry and topography grid, June 2009. Scale 1:5 000 000*. Canberra: Geoscience.
- Wilson, K. M., Allen, S. C. R., & Power, H. E. (2018). The tsunami threat to Sydney Harbour, Australia: modelling potential and historic events. *Scientific Reports*. <https://doi.org/10.1038/s41598-018-33156-w>.
- Wiśniewski, B., & Wolski, T. (2012). The safety of the shipping and ports in the aspect of the tsunami events. *Scientific Journals*, 30(102), 150–157.